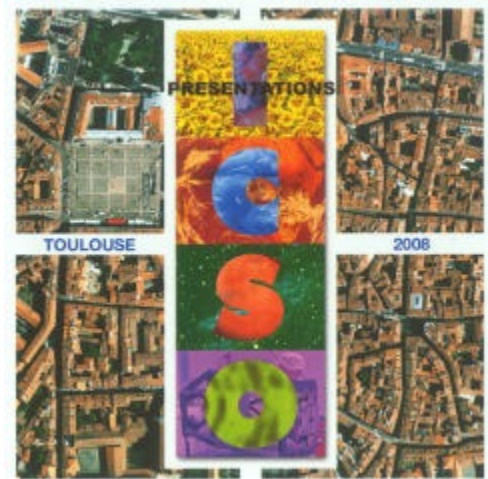


International Conference on Space Optics—ICSO 2008

Toulouse, France

14–17 October 2008

Edited by Josiane Costeraste, Errico Armandillo, and Nikos Karafolas



Instrument design and on-orbit performance of the solar optical telescope aboard hinode (Solar-B)

Yoshinori Suematsu

Kiyoshi Ichimoto

Yukio Katsukawa

Saku Tsuneta

et al.



INSTRUMENT DESIGN AND ON-ORBIT PERFORMANCE OF THE SOLAR OPTICAL TELESCOPE ABOARD HINODE (SOLAR-B)

Yoshinori Suematsu¹, Kiyoshi Ichimoto², Yukio Katsukawa¹, Saku Tsuneta¹ and Toshifumi Shimizu³

¹ National Astronomical Observatory of Japan, 2-21-1 Osawa, Mitaka, Tokyo 181-8588, Japan

E-mail: suematsu@solar.mtk.nao.ac.jp

² Kwasan and Hida Observatories, Kyoto University, Kurabashira, Takayama, Gifu 506-1314, Japan

³ Institute of Space and Aeronautical Science, JAXA, 3-1-1 Yoshinodai, Sagami-hara, Kanagawa 229-8510, Japan

ABSTRACT

The Solar Optical Telescope (SOT) aboard Solar-B satellite (Hinode) is designed to perform high-precision photometric and polarimetric observations of the solar lower atmosphere in visible light spectra (388--668 nm) with a spatial resolution of 0.2 to 0.3 arcsec. The SOT consists of two components; the optical telescope assembly (OTA) consisting of a 50-cm aperture Gregorian telescope with a collimating lens unit and an active tip-tilt mirror for an image-stabilization and an accompanying focal plane package (FPP) housing two filtergraphs and a spectro-polarimeter. Since its first-light observation on 25 Oct. 2006, the image-stabilization system has been working with performance better than 0.01 arcsec rms and the SOT has been continuously providing unprecedented solar data of high spatial resolution. Since the opto-mechanical and -thermal performance of the OTA is crucial to attain unprecedented high-quality solar observations, we here describe in detail the instrument design and on-orbit diffraction-limit performance of the OTA, the largest state-of-the-art solar telescope yet flown in space.

1. INTRODUCTION

The aim of the Solar Optical Telescope (SOT) aboard Solar-B satellite (post-launch nickname is Hinode) is to provide high-precision photometric and polarimetric data to investigate magnetic origins and mechanisms of active phenomena on the Sun. Additionally, the SOT is designed to explore the physical coupling between the photosphere and the upper layers to understand the mechanism of dynamics and heating with help of the coordinated observations of X-Ray Telescope [1][2] and EUV Imaging Spectrometer [3] flown on *Hinode* [4].

The SOT was designed to meet the following basic specifications: It should observe the field of view fully-covering a moderate sized active region of about 3×5 arcmin wide, with a spatial resolution corresponding to small-scale magnetic elements of 0.2--0.3 arcsec and with negligibly small and/or well-calibrated instrumental polarization [5][6][7][8]. The SOT comprises of very sophisticated instruments and consists of optically separable two components; the Optical Telescope Assembly (OTA) and the Focal Plane Package (FPP). This paper will focus on the OTA instrument design and its diffraction limited performance expected on-orbit.

2. OPTICAL DESIGN

The SOT was designed to achieve diffraction limit as a whole system. Following a conventional definition of the diffraction limit (Maréchal criterion, see [9], [10]), the goal was defined that the SOT has the Strehl ratio larger than 0.8 at 500 nm at the center of the field view, assuming of evenly budgeted Strehl ratios of 0.9 for both the OTA and the FPP. The Strehl ratio is a peak intensity of point source formed by a telescope normalized with the peak formed by a perfect telescope of no wavefront aberration. The Strehl ratio (SR) can be expressed with a root-mean-square (rms) wavefront error (WFE) by the relation:

$$SR = \exp[-(\frac{2\pi}{\lambda} WFE)^2]$$

and then the budget of OTA is 25.8 nm rms WFE, while the SOT has 36.5 nm rms. To achieve this goal, the budget was sub-divided for image-forming components and controlled during their fabrications and tests. The budget was also allocated for wavefront errors induced

requirements (2) and (3), was designed to be placed near the center of the primary mirror and to reduce beam size, making an exit pupil of 30 mm diameter to accommodate the clear apertures of the following polarization modulator and an active tip-tilt mirror for image stabilization. Afocal beam from the collimator lens is also of benefit to relax the positional tolerance for the FPP with respect to the OTA.

The distance between the primary and the secondary mirror was decided to be 1500 mm after considerable opto-mechanical tradeoff studies within the allowable size of the launcher's nosecone (maximum length ~ 2 m). Longer telescopes have an advantage to relax the positional tolerance of the secondary mirror. On the other hand, shorter telescopes can give better mechanical stability and also require smaller secondary mirror (central obscuration) and hence better image contrast for observing of solar granulation.

Then, the idea was that the OTA should be a Gregorian with the Collimating Lens Unit (CLU) near the center of the primary mirror, followed by a Polarization Modulator Unit (PMU), and an active Tip-Tilt Mirror (CTM-TM). In addition, the OTA has two field stops in between the primary and secondary mirror; one is a heat dump mirror (HDM) at a focus of the primary mirror and the other is a secondary field stop (2FS) at the Gregorian focus. Besides the above-mentioned requirements, more practical requirements given below finally determined the basic optical parameters of OTA: 1) The Gregorian should be aplanatic (both spherical and coma aberration free) to give better image quality over the specified wide FOV. 2) An entrance pupil was positioned 200 mm in front of the secondary mirror vertex. 3) A principal point of CLU was positioned 50 mm beneath the vertex of primary mirror and the 30 mm diameter exit pupil formed 300 mm below the CLU, around which moving optical elements, PMU and CTM-TM were located. 4) The HDM outer diameter is about twice of diameter of the solar image at the primary focus so that it allows an offset pointing of the telescope for solar limb observations up to 200 arcsec off the limb. 5) The HDM has a through hole passing the beams of field of view 500 arcsec diameter (400 arcsec plus 0.3 mm margin)

and it should not vignette any beams reflected back from the secondary mirror with a clear margin of at least 0.5 mm. Derived optical parameters are given in [6] and the optical layout of the OTA is shown in Fig. 1.

3. MECHANICAL AND THERMAL DESIGN

The framework structure of OTA should be light weight but sufficiently robust to support and maintain the optical elements with a required positional accuracy against a violent launch environmental conditions and severe on-orbit thermal conditions without any dedicated alignment mechanisms. The SOT has a single focusing (re-imaging) mechanism at the entrance of the FPP.

The Gregorian OTA requirements demand very small static mis-alignment tolerances for the primary and secondary mirrors, on the order of a few tens microns for de-center and de-space or several arcsec for tilt, and a micron-order de-space short-term stability on-orbit during observations. To meet this requirement, the telescope framework was made of a truss of newly-developed ultra-low-expansion CFRP (Carbon Fiber Reinforced Plastics) pipes in a Graphite Cyanate matrix [13]. The CTE was proven to be smaller than ± 0.1 ppm K^{-1} , and the dimensional change due to moisture absorption was measured to be about 30 ppm which is much smaller than conventional epoxy matrix composite pipes. Three CFRP honeycomb sandwich panels (rings) were adhesively bonded with upper and lower truss pipes without any metal junctions to save weight and also avoid differential CTE which may cause unexpected telescope thermal distortion.

A layout of overall the OTA structural assembly is shown in Fig. 2. The center panel ring (called center section) provides the mechanical interface to the spacecraft; OTA is mounted on the CFRP-made cylindrical optical bench unit (OBU) to the spacecraft with three quasi-kinematic titanium alloy mounting legs with stress-relief spring structures. The center section is equipped with alignment cubes at the top surface which represent the mechanical and optical axes of the OTA, and are used for co-alignment among other telescopes and spacecraft attitude control system sun-sensors.

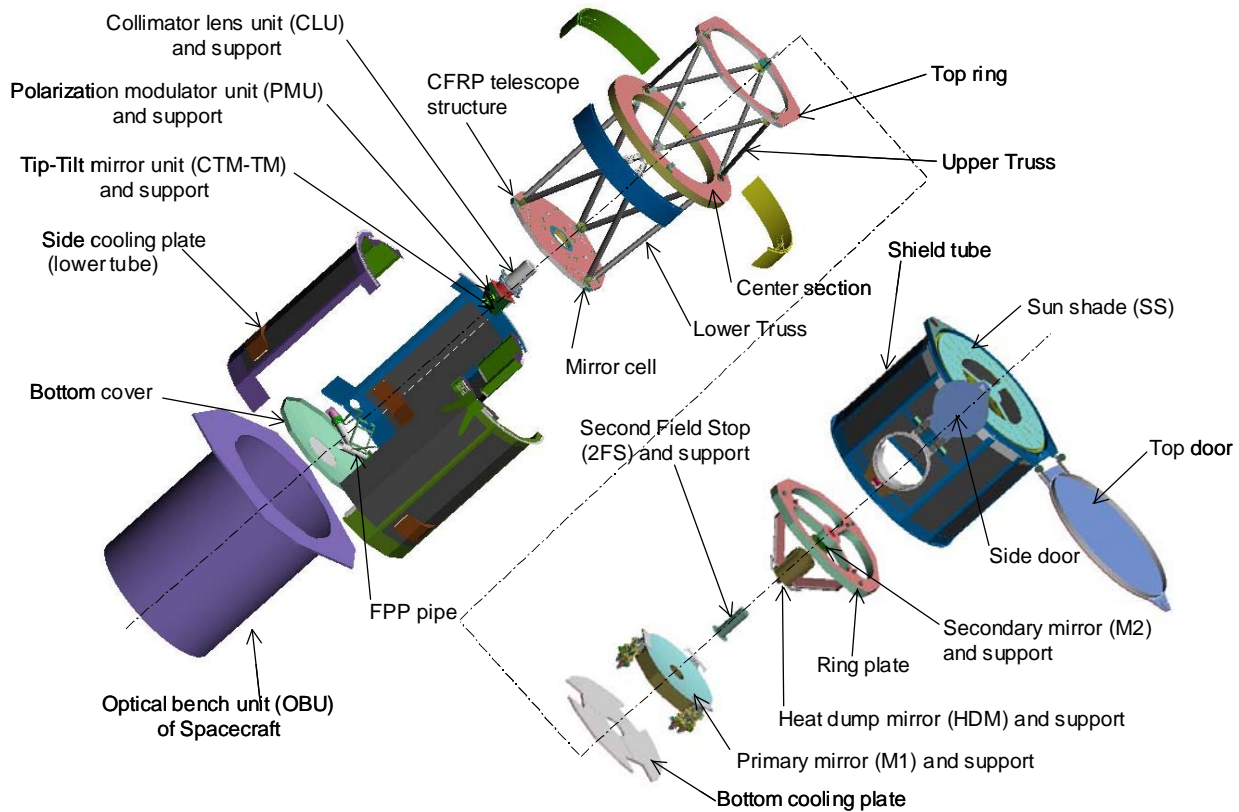


Fig. 2. Layout of the OTA structural assembly.

Mounting of the primary mirror is one of the most critical parts of the OTA. The primary mirror, made of light-weighted (70% removed and thus 14 kg weight) ULE, is supported by three stress-free mounting mechanisms seated on the CFRP bottom panel (called mirror cell), interfaced with three superinvar pads bonded on the side of the mirror. The pad interface of the mounting mechanism is torque-free about three axes and also free in the radial direction, thus providing a kinematic mount for the primary mirror. The pad interface thus avoids stresses to the mirror resulting from dimensional errors in machining or temperature change. The only significant surface error of the primary mirror is caused by the difference of CTE between the superinvar pads and the ULE, which constrains the best-performance temperature range of the primary mirror to be between -15 to 55 degC.

Titanium cylinders housing the CLU and PMU and supporting CTM-TM aft end are also tightly mounted on the mirror cell, whose positional tolerances are relatively loose, after the secondary mirror is optically aligned with

the primary. The secondary mirror, which is also made of ULE shaped like a Japanese large flat winecup, is supported by a superinvar tripod-shaped pad of stress relief spring legs which are glued at the side of M2 backside cylindrical hump. The pad located on the opposite side of M2 is bolted to the central part of another CFRP panel ring with spiders (called ring plate). The surface error of the secondary mirror can be again caused by the CTE difference between the superinvar pad and the ULE, and it constrains the best-performance temperature range between 0 to 40 degC.

The HDM unit is also supported by the ring plate via three mounting spiders made from honeycomb panel (aluminum core and CFRP skin). The mounting points at the ring plate have a titanium-made mechanism for de-center and tilt adjustment of HDM unit with respect to M2 and HDM. The HDM has through hole through which the HDM can be properly aligned with a fiducial at the M2 vertex. The ring plate is connected to the CFRP top panel ring via three positional and tilt adjustment mechanisms made of superinvar rods, with

which optical alignment of the secondary mirror, de-center, de-space (focus), and tilt adjustment with respect to the primary mirror can be performed. OTA is covered by a shield tube for the upper half and a lower tube for the lower half for the purpose of protecting critical components from molecular and particle contamination, as well as reducing stray light, and ensuring thermal control of the entire OTA. The shield tube is made of aluminum honeycomb sandwich plates and also provides a structural support of a top and side door, and a sunshade defining the entrance pupil of OTA.

About 210 W of solar light is inevitably impinged onto the primary mirror at the bottom of the OTA during solar observations from its 500 mm diameter entrance aperture. The lower half of the OTA is inserted into the cylindrical OBU which provides a stable and isotropic thermal environment for the primary mirror. As a result, there is no short path to dump the heat absorbed by the primary mirror to space. A thermal design to dump such a large heat load to space and maintain critical optical and structure components to within allowable temperature ranges with small temperature fluctuation is critically important to realize a high-performance solar telescope. The operational (best performance) primary and secondary mirror temperature ranges shown above are required to maintain on-orbit OTA performance,

From this viewpoint, the coating design of optical components is critical, which should limit solar light absorptance to a minimum, giving high throughput in the observation wavelengths and rejecting light outside their wavelengths (IR and UV). The protected silver coating of M1 and M2 contributed a small solar absorptance of 6.5%, while the enhanced silver coating of the HDM and 2FS contributed a lesser solar absorptance of 6.1%; actual absorptances for HDM and 2FS are 3.9% after M1 and 3.6% after M1 plus M2 reflection, respectively. The first surface of the CLU has the multi-layer coating for IR/UV rejection. The shape of the first surface of the CLU is concave with its center of curvature coinciding with the center of the secondary field stop. Thus, the CLU acts as an IR blocking filter with the reflected light through the secondary field stop. It is noted that the major fraction of rejected light by the secondary field

stop and the CLU can escape to space through the entrance aperture of the OTA. The CTM-TM mirror has the optimized enhanced silver coating for a 45 deg. incidence and hence has small solar absorptance.

Based on the predicted orbit of Hinode, extreme cases were defined and studied for OTA thermal design; 'cold case' (solar limb observation in the coldest orbit with measured absorptance at the beginning of life) and 'hot case' (solar disk center observation in the hottest orbit with absorptance assumed by 5% increase toward the end of life). The basic concept of the OTA thermal design can be summarized as follows:

- 1) Most incident energy (165 - 185W) coming inside the OTA is reflected back by the primary mirror and dumped out to space by the HDM at the primary focus through the heat dump window opened at the side of the OTA.
- 2) The sunshade and upper half of the shield tube work as a thermal radiator. The sunshade has an optical solar reflector facing the Sun to keep it cold, while the upper area of the shield tube, not covered by multi-layer insulation (MLI), is covered with a silverized teflon sheet; a good IR radiator.
- 3) Solar heat (13 - 24 W) absorbed by the primary mirror is radiatively transmitted to the lower tube from its side and from a bottom cooling plate just beneath the mirror. The bottom cooling plate consists of a gold-plated aluminum honeycomb sandwich panel and radiatively absorbs the heat of the mirror from its back face. De-contamination heaters are attached to the back side of the bottom cooling plate.
- 4) Solar heat (~ 1.5 W) absorbed by the secondary mirror is radiatively transmitted to the radiators from its back side.
- 5) Heat (~ 2 W) absorbed by the 2FS, CLU, PMU and CTM-TM and generated by their electronic components is conductively transferred to the mirror cell and also emitted out through their housings, and is finally radiatively transmitted to the lower tube.
- 6) Heat (10 - 20 W) of the HDM is conductively transferred to the cylindrical structure supporting the HDM and outer spiders connecting the ring plate, and then radiatively transferred to the shield tube, the radiator and space through the heat dump window.
- 7) The heat of the lower tube and the shield tube is

radiatively emitted directly to the 3K temperature of space through the entrance pupil and indirectly via the radiator of the sunshade and upper shield tube.

8) The OTA is thermally insulated from the spacecraft; The OTA is physically connected to the OBU only by the three mounting legs of low-thermally conductive titanium and is radiatively de-coupled from the OBU by MLI covering the lower tube and the bottom cover.

9) In the cold phase (e.g. solar limb observations), the secondary mirror and CLU are warmed and maintained at their operational temperatures by dedicated operational heaters. The heater for the secondary mirror is attached to a separate heater plate behind the mirror, and for the CLU is attached to the bottom cover. They warm up the optical elements indirectly by radiation to prevent localized temperature gradients and temperature ripples of optical elements due to the heater duty cycles.

10) In the post-launch coldest phase, the critical optics are protected with survival heaters and later with de-contamination heaters so that the temperature of the optics can be maintained by about ten Centigrade higher than their surrounding structures. Especially, the top and side doors are designed to work as cold plates, the coldest surfaces inside the OTA, absorbing out-gassing contaminants. Note that the side door should open before the top door to allow out-gassing contaminants to escape away from the heat dump window.

4. GROUND TESTING AND ON-ORBIT PERFORMANCE

We measured the wavefront error using an interferometer after integrating the CLU, PMU, CTM-TM and ACL to the OTA (+1 G condition). The interferometer sent a collimated beam into the OTA from the exit pupil. With the folding flat above the entrance pupil, the double-path wavefront error of the OTA was obtained. In the interferometer measurements, we employed a technique for deriving the phase (wavefront error) from a single interferogram (taken with a short exposure of 8 msec) using spatial heterodyning with high tilt of a reference flat. This method is less affected by the vibration of the test set-up and the change in seeing conditions through a long optical path. In addition, the wavefront error of the interferometer itself was calibrated.

We carefully corrected phase unwrappings and phase gaps between three sections divided by the three spiders in restoring the phase from the interferogram. Typically, hundreds of usable interferograms, which were manually obtained, were used to achieve an accuracy of 5 nm rms for a single path. To calibrate a non-axi-symmetric wavefront error of the folding flat mirror (confirmed small axi-symmetric aberration in the flat mirror alone test), we measured four sets of wavefront errors by rotating the flat by 90deg steps around its axis and took their average. The result is given in Fig. 3.

Finally, rotating the OTA upside-down and setting the interferometer and the flat mirror for this configuration, we performed the measurements for a -1 G condition. By averaging the -1 G and the +1 G wavefront, the effect of gravity can be canceled out and the OTA wavefront error in this zero-gravity condition was reduced. During these activities, mutual angles between the OTA pointing axis, exiting beam axis and mechanical axis were measured by correlating the tilt of the folding flat mirror, image of the secondary field stop in exiting beam, and the alignment cube, respectively.

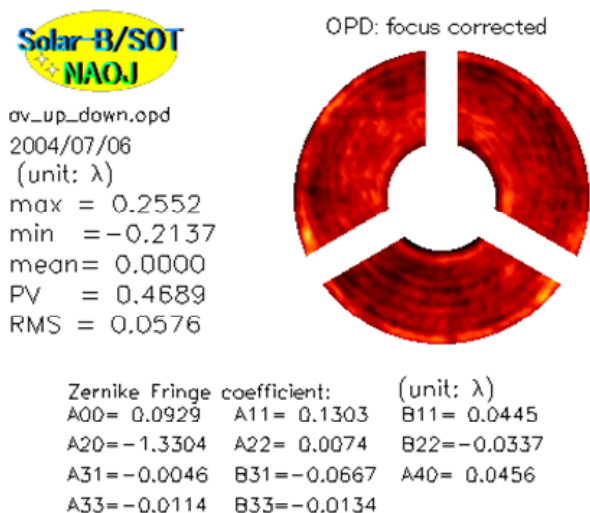


Fig. 4. The wavefront error map of the OTA for the zero-gravity condition.

The thermal model predicts that the OTA on orbit will inevitably have a large temperature gradient along the optical axis; the bottom part of telescope including the primary mirror will reach a temperature of +24 to +47degC, while the upper structures supporting the

secondary mirror will reach a temperature of 9 to 30degC, depending on thermal conditions and its life phase. We verified the optical performance in such a temperature distribution even though the opto-mechanical design predicts that those temperatures are acceptable.

The OTA optical performance was repeatedly verified with several post-environmental test interferometer measurements for the OTA alone and the satellite until just before the launch. The wavefront error of OTA has not changed within the measurement error of several nm rms, when removing defocus error. We observed monotonic change in focus over months which can be explained with an expansion of CFRP truss pipes connecting M1 with M2 by moisture absorption in air. This expansion will be mostly canceled by dehydration shrinkage of pipes on-orbit.

Following the successful launch of the satellite on 23rd September, 2006 (JST), the SOT had a first-light by the deployment of the OTA top door on 25th October, 2006. Note that the side door had been opened eleven days before with de-contamination heaters enabled for M1, M2 and HDM so that OTA structure outgassing, a source of contaminants, could well escape through the heat dump window.

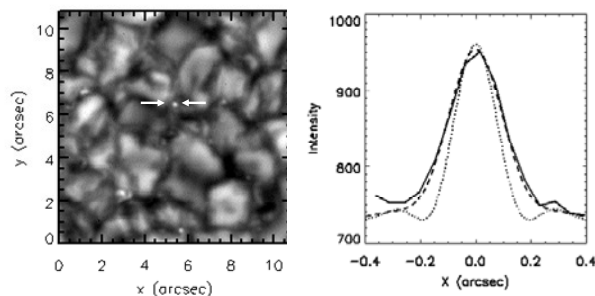


Fig. 4. First light image in the G-band (430 nm) and the optical performance of the OTA.

The first-light images were taken with FPP G-band (430 nm) filtergraph during the door deployment. Then a focus scan was performed at the disk center of the Sun to have the best focus position of the focusing (re-imaging) lens, after the SOT temperatures stabilized. An example of the G-band images in focus is shown in Fig. 4. Note that the correlation tracker image stabilization system

was not yet used at this time. Nevertheless, the G-band images are superb, showing many point-like bright features of about 0.2 arcsec wide. To check the resolution, the intensity profile of the point-like bright features was compared with an ideal point spread function (PSF) of OTA as shown in Fig. 4. The profile of the bright point can be explained if its true profile is a 2-D Gaussian of 0.16 arcsec FWHM; the profile convolved of the PSF with the Gaussian gives the observed one. The bright point 0.16 arcsec wide makes sense and this implies that the G-band filtergraph of SOT has the diffraction-limited performance. Therefore, there is no doubt that the OTA keeps the superb diffraction-limited performance on orbit.

5. SUMMARY

We have described in detail the instrument design and ground testing of the Optical Telescope Assembly (OTA) of the Solar Optical Telescope (SOT) aboard the *Hinode* satellite. As the first-light images from the SOT have demonstrated, it started continuously providing unprecedented solar optical data of high spatial resolution. It is concluded that the OTA is the largest state-of-the-art solar telescope that has ever been completed and flown in space.

REFERENCES

1. Golub, L., et al., 2007, Solar Phys. **243**, 63.
2. Kano, R., et al., 2008, Solar Phys. **249**, 263.
3. Culhane, J.L., et al., 2007, Solar Phys. **243**, 19.
4. Kosugi, T., et al. 2007, Solar Phys. **243**, 3.
5. Tsuneta, S., et al. 2008, Solar Phys. **249**, 167.
6. Suematsu, Y. et al., 2008, Solar Phys. **249**, 197
7. Shimizu, T., et al., 2008, Solar Phys. **249**, 221.
8. Ichimoto, K., et al., 2008, Solar Phys. **249**, 233.
9. Schroeder, D. J., 2000, Astronomical Optics, 2nd ed., Academic Press, San Diego.
10. Wilson, R. N., 1996, Reflecting Telescope Optics I, Springer, Berlin.
11. Dunn, R. B., 1981, Space Science Rev. **29**, 341.
12. Title, A. M., 1989, in von der L uhe, O. (ed.), High Spatial Resolution Solar Observations, Proc. 10th Sac Peak Summer Workshop, NSO, 35.
13. Ozaki, T., et al., 1996, in Rust, D.M. (ed.), Missions to the Sun, Proc. SPIE **2804**, 22.